Lattice Gas Monte Carlo Study on the Cassie–Baxter to Wenzel Transition of the Water Droplet Deposited on Parabolic Pillars

Hyojeong Kim,† Mohammad A. Matin,† Yeongmin O, Jihye Jang, Zhengqing Zhang, and Joonkyung Jang*

*Department of Nanomaterials Engineering and BK21 Plus Nano Convergence Technology Division, Pusan National University, Busan 609-735, Republic of Korea. *E-mail: jkjang@pusan.ac.kr*
Received November 13, 2014, Accepted November 18, 2014, Published online January 15, 2015

Keywords: Wenzel, Cassie–Baxter, Lattice gas Monte Carlo, Super-hydrophobic surface

Over the years, surfaces patterned with periodic pillars have been utilized as super-hydrophobic surfaces. Such pillared surfaces are applicable for self-cleaning,[1] drag reduction,[2,3] coating,[4] and microfluidics, just to name a few.[5] Given micro- or nano-pillars of various sizes and shapes that can be patterned these days, efforts have been made to find the optimal geometry of a pillared surface that exhibits maximal hydrophobicity. A surface patterned with parabolic pillars is particularly interesting because of its resemblance to a lotus leaf, which is well known for its super-hydrophobicity.[6]

The hydrophobicity of a pillared surface is commonly assessed by examining whether a water droplet resting on it penetrates down into the gap between the pillar walls. The former and latter cases, respectively, are taken to be the Cassie–Baxter[7] (CB) and Wenzel[8] (WZ) states of the droplet (Figure 1). Typically, the CB-to-WZ transition is induced by increasing the spacing S between the pillars or by raising the pressure P of the droplet.

Using theory and Monte Carlo (MC) simulation, we previously studied the CB-to-WZ transition for the surfaces covered with rectangular, cylindrical, and parabolic pillars.[9,10] Interestingly, with increasing S or P, the water droplet penetrated down into the gap between parabolic pillars smoothly from the top to the bottom of the pillars.[10] This contrasts with the abrupt penetration (at a critical value of S or P) into the gap between rectangular or cylindrical pillars, which is characteristic of a first-order phase transition.

Currently, it is unclear whether the smooth intrusion of the droplet into the gap between the parabolic pillars will be valid when the parabolic pillars become tall and sharp like needles. Here, we investigate the CB-to-WZ transition for various aspect ratios of parabolic pillars. By employing the lattice gas MC (LGMC) simulation, we continuously changed S or P to observe the CB-to-WZ transition. The present LG model is a minimal molecular model that captures the essence of the phase transition of a confined water droplet. A detailed description of the present LGMC simulation can be found in our previous work.[9–11]

Plotted in Figure 1(c) is the average density $<\rho>$ of the water confined between the parabolic pillar walls as a function of S. Regardless of the aspect ratio H/W of the pillar (ranging from 2 to 10), the density smoothly increased from a near-zero value (vapor phase) to a value close to 1 (liquid phase) as S increased from 0.7 to 8.9 nm. This smooth increase in the density is distinctly different from the step-like jump at a critical value of S found for the gap between the rectangular or cylindrical pillar walls. Even quantitatively, the $<\rho>$ *vs.* S curves almost overlap with each other. Small differences exist, however. The liquid densities for large S values were slightly larger for higher values of H. On the other hand, the vapor densities at small values of S slightly decreased with increasing H. The turnover behavior in the relative magnitudes of the densities for different H values occurred at approximately $S = 6.3$ nm.

We examined how the pressure P affects the CB or WZ state of the water droplet. Figure 2(a) shows $<\rho>$ *vs.* P for the water trapped between the parabolic pillars for $S = 4.4$ nm and $W = 11.8$ nm. The height H of the pillar varied from 23.7 to 118.4 nm. As P was increased from 0 to 8 MPa (with an increment of 0.5 MPa), $<\rho>$ gradually (almost linearly) increased, owing to the smooth invasion of the droplet down into the inter-pillar gap. Here again, the CB-to-WZ transition contrasts with that found for the rectangular or cylindrical pillars, which exhibited a discontinuous jump at a critical value of P.

Of particular interest is how vulnerable the gap between the pillar walls is to the increase in P. This is quantified by the slope of the $<\rho>$ *vs.* P curve, which is called the pressure susceptibility in the present work. The pressure susceptibility is plotted *vs.* P in Figure 2(b) (drawn as circles). The susceptibility does not have any conspicuous peak characteristic of a first-order transition. Instead, the susceptibility is broadly distributed, with a small shoulder located around 7 MPa. We demonstrate that the pressure susceptibility is related to the fluctuation of the density, $\langle(\delta\rho)^2\rangle \equiv <\rho^2> - <\rho>^2$, where $<\rho^2>$ is the average of the density squared. Using the statistical mechanical relation $<(\delta\rho)^2> = (k_BT/N)(\partial\langle\rho\rangle/\partial\mu)$, where N is the number of total lattice sites of the inter-pillar gap,[12] we can write

$$\partial\langle\rho\rangle/\partial P = (N/\rho_b k_B T) <(\delta\rho)^2> \quad (1)$$

† These authors contributed equally to this work.

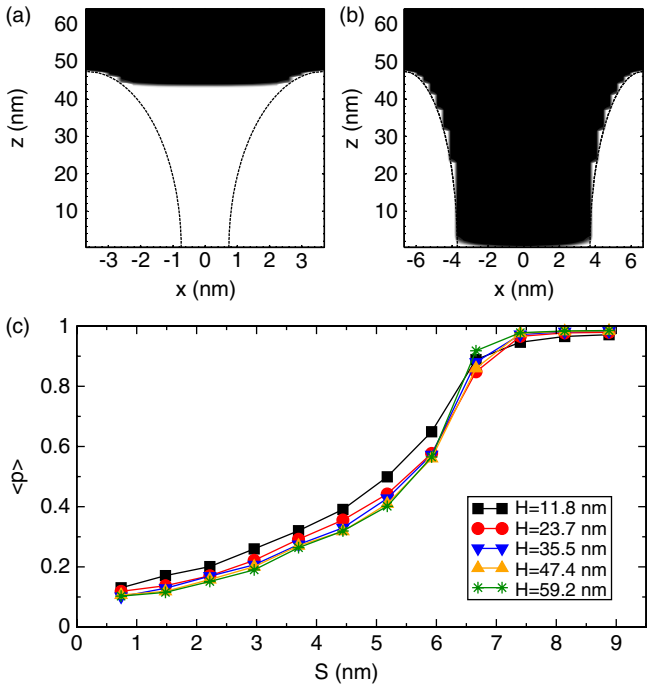

Figure 1. Snapshots of the Cassie–Baxter (a) and Wenzel (b) states of a macroscopic water droplet sitting on a surface covered with parabolic pillars. Shown are the cross-sectional snapshots taken along the planes that vertically dissect the pillars into half (in this case, the *XZ* plane). For a fixed pillar height *H* of 47.4 nm, the inter-pillar spacing *S* was varied as 1.5 (a) and 7.4 (b) nm. *S* refers to the distance between the bottoms of the neighboring pillars. In simulation, the parabolic pillars were periodically replicated on a square grid. Mean density of the water confined in the gap between the pillars $<\rho>$ *vs.* the inter-pillar spacing *S* (c). The height of pillar *H* was varied from 11.8 to 59.2 nm by fixing the width *W* to 5.9 nm. *W* refers to the width of each pillar at its bottom. *P* was fixed to 4 MPa.

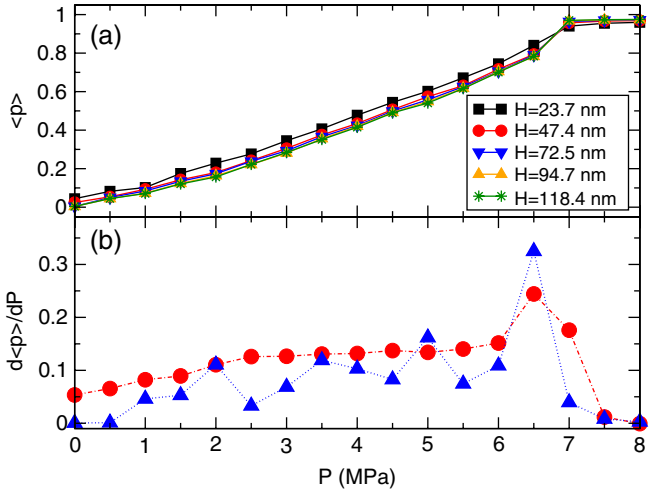

Figure 2. (a) Pressure dependence of the density of the water confined between parabolic pillar walls. By fixing *S* and *W* to 4.4 and 11.8 nm, respectively, we continuously varied the pressure from 0 to 8 MPa. The average density $<\rho>$ *vs.* *P* is shown for different *H* ranging from 23.7 to 118.4 nm. (b) Pressure susceptibility of the density *vs.* the pressure *P*. The susceptibilities obtained from evaluating $d<\rho>/dP$ numerically and from using the fluctuation, Eq. (1), are drawn as circles and triangles, respectively. *H* was fixed at 47.4 nm. Lines serve as visual guide.

here, we further used the approximation $d\mu = (1/\rho_b)dp$, where ρ_b is the bulk density. Therefore, the pressure susceptibility is proportional to the fluctuation in the density of the inter-pillar gap. Using the LGMC simulation result, we calculated the susceptibility from the density fluctuation, drawn as triangles in Figure 2(b). The susceptibilities by using the numerical derivatives (circles) sensibly agree with those by using the fluctuation expression, Eq. (1).

In conclusion, we have studied how a water droplet sitting on top of parabolic pillars penetrates down into the gap between the parabolic pillar walls as the spacing between the pillars or the pressure of droplet was increased. This penetration pertains to the CB-to-WZ transition of the droplet. By using the LGMC simulation, we simulated pillars with various shapes ranging from dome-shaped to needle-like. Regardless of the shape, the penetration between the parabolic pillar walls was always smooth, which is in stark contrast to the abrupt filling found for the gap between rectangular or cylindrical pillars. This smooth behavior was also found for the CB-to-WZ transition induced by increasing the pressure of the droplet. We related the pressure susceptibility of the density of the water confined between the pillar walls to the fluctuation in the density of the confined water.

Acknowledgment. This work was supported by a 2-year Research Grant of Pusan National University.

References

1. R. Blossey, *Nat. Mater.* **2003**, *2*, 301.
2. J. Ou, B. Perot, J. P. Rothstein, *Phys. Fluids* **2004**, *16*, 4635.
3. P. Joseph, C. Cottin-Bizonne, J. M. Benoît, C. Ybert, C. Journet, P. Tabeling, L. Bocquet, *Phys. Rev. Lett.* **2006**, *97*, 156104.
4. I. P. Parkin, R. G. Palgrave, *J. Mater. Chem.* **2005**, *15*, 1689.
5. K. Tsougeni, D. Papageorgiou, A. Tserepi, E. Gogolides, *Lab Chip* **2010**, *10*, 462.
6. W. Barthlott, C. Neinhuis, *Planta* **1997**, *202*, 1.
7. A. B. D. Cassie, S. Baxter, *Trans. Faraday Soc.* **1944**, *40*, 546.
8. R. N. Wenzel, *Ind. Eng. Chem.* **1936**, *28*, 988.
9. H. Kim, J. K. Saha, J. Jang, *J. Phys. Chem. C* **2012**, *116*, 19233.
10. H. Kim, S. I. Lee, M. A. Matin, Z. Zhang, J. Jang, M. Y. Ha, J. Jang, *J. Phys. Chem. C* **2014**, *118*, 26070.
11. J. Jang, G. C. Schatz, M. A. Ratner, *Phys. Rev. Lett.* **2004**, *92*, 085504.
12. T. L. Hill, *Statistical Mechanics: Principles and Selected Applications*, Dover Publications, New York, 1987.

